AD NUMBER

AD830407

LIMITATION CHANGES

TO:

Approved for public release; distribution is unlimited.

FROM:

Distribution authorized to U.S. Gov't. agencies and their contractors; Critical Technology; APR 1968. Other requests shall be referred to Air Force Office of Scientific Research, Attn: SREM, Arlington, VA 22209. This document contains export-controlled technical data.

AUTHORITY

AFOSR ltr, 1 Oct 1972

AEROELASTIC STABILITY TESTS OF THIN CYLINDRICAL SHELLS AT SUPERSONIC SPEEDS

T. R. Brice

ARO, Inc.

April 1968

PROPULSION WIND TUNNEL FACILITY
ARNOLD ENGINEERING DEVELOPMENT CENTER
AIR FORCE SYSTEMS COMMAND
ARNOLD AIR FORCE STATION, TENNESSEE

NOTICES

When U. S. Government drawings specifications, or other data are used for any purpose other than a definitely related Government procurement operation, the Government thereby incurs no responsibility nor any obligation whatsoever, and the fact that the Government may have formulated, furnished, or in any way supplied the said drawings, specifications, or other data, is not to be regarded by implication or otherwise, or in any manner licensing the holder or any other person or corporation, or conveying any rights or permission to manufacture, use, or sell any patented invention that may in any way be related thereto.

Qualified users may obtain copies of this report from the Defense Documentation Center.

References to named commercial products in this report are not to be considered in any sense as an endorsement of the product by the United States Air Force or the Government.

AEROELASTIC STABILITY TESTS OF THIN CYLINDRICAL SHELLS AT SUPERSONIC SPEEDS

T. R. Brice
ARO, Inc.

AF—AEDC
Arnold AFS Tenn

FOREWORD

The work reported herein was done at the request of the Aerospace Engineering Department of the University of Texas for the Air Force Office of Scientific Research (AFOSR), Air Force Systems Command (AFSC), under Program Element 6144501F, Project 9782.

The results of the test presented were obtained by ARO, Inc. (a subsidiary of Sverdrup & Parcel and Associates, Inc.), contract operator of the Arnold Engineering Development Center (AEDC), AFSC, Arnold Air Force Station, Tennessee, under Contract AF40(600)-1200. The test was conducted from October 24 through November 2, 1967, and from January 15 through 19, 1968, under ARO Project No. PS0833. The manuscript was submitted for publication on March 19, 1968.

Information in this report is embargoed under the Department of State International Traffic in Arms Regulations. This report may be released to foreign governments by departments or agencies of the U. S. Government subject to approval of the Air Force Office of Scientific Research (SREM), or higher authority within the Department of the Air Force. Private individuals or firms require a Department of State export license.

This technical report has been reviewed and is approved.

Richard W. Bradley
Lt Colonel, USAF
AF Representative, PWT
Directorate of Test

Roy R. Croy, Jr.
Colonel, USAF
Director of Test

ABSTRACT

Dynamic characteristics of thin cylindrical shells were investigated for Mach numbers from 2.2 to 3.0. The Reynolds number based on the model diameter varied from 0.34 to 2.58 million. Limit cycle oscillations in a standing wave mode occurred on a 0.0020-in. shell at Mach number 2.2. The limit cycle motion was damped completely by blowing air into the boundary layer at a very low rate. A 0.0028-in. shell was destroyed during high amplitude oscillations at Mach number 2.2. Pressure distribution and boundary-layer measurements were also made.

CONTENTS

		Page
	ABSTRACT	iii
	NOMENCLATURE	vi
I.	INTRODUCTION	1
II.	APPARATUS	
	2.1 Wind Tunnel	1
	2.2 Test Article	1
	2.3 Instrumentation	3
III.	TEST PROCEDURE	
	3.1 Pressure Phase	4
	3.2 Flutter Phase	5
	3.3 Precision of Measurements	5
IV.	RESULTS	
	4.1 Pressure Phase	6
	4.2 Flutter Phase	7
V.	CONCLUSIONS	9
	REFERENCES	9

TABLES

I.	Summary of Test Conditions	7
II.	Flutter Conditions	8

APPENDIX

Illustrations

Figure		
1.	Variations of Tunnel Reynolds Number with Mach Number	13
2.	Sketch of the Model in the Tunnel 16S Test Section	14
3.	Photograph of the Model Installed in the Tunnel 16S Test Section	15
4.	Model Dimensions and Details	16
5.	Details of the Test Panel	17
6.	Details of the Boundary-Layer Rakes	18

Figure		Page
7.	Sketch of the Traversing Rake (Rake 3)	19
8.	Photographs of Rake 3	
	a. Forward Position	20
	b. Aft Position	21
9.	Variation of Pressure Coefficients on the Test Shell, with and without Boundary-Layer Blowing	
	a. $M_\infty = 2.20$	22
	b. $M_\infty = 3.00$	23
10.	Boundary-Layer Profiles at x/L = 1.00	
	a. $M_\infty = 2.20$, Re/ft = 0.564×10^6	24
	b. $M_\infty = 2.20$, Re/ft = 1.092×10^6	25
	c. $M_\infty = 2.20$, Re/ft = 1.546×10^6	26
	d. $M_\infty = 3.00$, Re/ft = 0.560×10^6	27
	e. $M_\infty = 3.00$, Re/ft = 0.994×10^6	28
	f. $M_\infty = 3.00$, Re/ft = 1.289×10^6	29
11.	Effect of Reynolds Number and Blowing on the Boundary-Layer Thickness at x/L = 1.00	
	a. $M_\infty = 2.20$	30
	b. $M_\infty = 3.00$	30
12.	Variation of the Displacement Thickness along the Model Surface, with and without Boundary-Layer Blowing	
	a. $M_\infty = 2.20$, Re/ft = 0.564×10^6	31
	b. $M_\infty = 2.20$, Re/ft = 1.546×10^6	31
	c. $M_\infty = 3.00$, Re/ft = 1.289×10^6	31

NOMENCLATURE

BLC	Boundary-layer control
C_p	Pressure coefficient, $\dfrac{p - p_\infty}{q_\infty}$
D	Model reference diameter, 1.333 ft
E	Young's modulus of elasticity, 2.736×10^9, psf
$\bar{F}$	Flutter parameter, $\left(\dfrac{q_\infty}{E\sqrt{M_\infty^2 - 1}} \right)^{1/3} \dfrac{R}{h}$

h	Shell thickness, in.
L	Shell reference length, 1.333 ft
M_ℓ	Local Mach number
M_∞	Free-stream Mach number
p	Pressure measured on the test shell, psf
p_c	Cavity pressure beneath the shell, psi
p_{t_∞}	Free-stream total pressure, psf
p_∞	Free-stream static pressure, psf or psi
q_∞	Free-stream dynamic pressure, psf
R	Shell radius, 8.00 in.
Re	Reynolds number per foot, $\frac{V_\infty}{\nu_\infty}$
U	Velocity outside the boundary layer, ft/sec
u_ℓ	Local velocity, ft/sec
V_∞	Free-stream velocity, ft/sec
$\dot{w}$	Weight flow into boundary layer, lb/sec
x	Distance from the forward edge of the test shell (Fig. 5), in.
y	Distance measured normal to the model surface, in.
Δp_c	Differential pressure across the shell, $(p_c - p_\infty)$, psi
δ	Boundary-layer thickness, in.
δ^*	Boundary-layer displacement thickness, in., $\int_0^\delta \left(1 - \frac{\rho_\ell u_\ell}{\rho U}\right) dy$
ν_∞	Free-stream kinematic viscosity, ft^2/sec
ρ	Density outside the boundary layer, $slugs/ft^3$
ρ_ℓ	Local density, $slugs/ft^3$
ϕ	Rotational angle measured on the model (Figs. 4 and 5), deg

SECTION I
INTRODUCTION

As monocoque structures are being used widely in all missile and launch vehicle stages, more information about the dynamic characteristics under various load conditions and external flow fields is mandatory. The cylindrical shell flutter model was tested to determine the effects of differential pressure, axial loading, and boundary-layer blowing on the flutter of thin wall, cylindrical shells.

The testing was conducted in the Propulsion Wind Tunnel, Supersonic (16S) in two phases. The first phase served to define the static pressure distributions and boundary-layer characteristics with control conditions varied. The purpose of the second phase was to investigate the dynamic properties of the shells. The Mach number range was from 2.2 to 3.0 (Fig. 1, Appendix), and the model was tested at zero angle of attack for both phases.

An earlier test conducted in the Propulsion Wind Tunnel, Transonic (16T) has been documented in Ref. 1. The test shells of Ref. 1 were made to flutter by reducing the cavity pressure. During flutter and before failure of several shells, spirally traveling waves were observed.

SECTION II
APPARATUS

2.1 WIND TUNNEL

Tunnel 16S is a variable density wind tunnel capable of operating at Mach numbers from 1.70 to 3.10. The test section is 16 ft square and is composed of two 20-ft-long removable sections. A more complete description of the tunnel may be found in Ref. 2, and calibration results are presented in Refs. 3 and 4. A sketch of the model installed in the test section is presented in Fig. 2, and a photograph of the model is presented in Fig. 3.

2.2 TEST ARTICLE

The cylindrical shell model, with different test shells, was used in both the pressure and flutter phases and is detailed in Fig. 4. The test shell (Fig. 5) was located on the cylindrical portion of the model, 96 in.

downstream of the model nose. For the Reynolds numbers involved, the test shell was assured to be in a region of a developed turbulent boundary layer. The aft edge of the test shell was held in place by the support section, which was mounted to the tunnel sting by a dummy balance. A rigid tube passed through the shell and mated to a flange which supported the upstream end of the shell. The boundary-layer control section bolted to the flange and housed the upstream axial bladder which contacted the shell end ring. The ogive-cylinder section then bolted directly to the boundary-layer control section.

The effect of boundary-layer blowing on the static pressure distribution and boundary-layer profiles over the shell and the dynamic characteristics of the shell were investigated by injecting heated nitrogen into the external flow. Cold nitrogen was heated in the tunnel plenum chamber and piped through the model base, to a manifold which emptied the nitrogen into the free steam through a 0.065-in. circumferential slot. The slot was located 72 in. downstream of the model nose. The upstream pressures in the boundary-layer duct and the slot width resulted in blowing rates up to 0.40 lb/sec.

Effects of the boundary-layer blowing were determined by pressure measurements on three boundary-layer rakes (Figs. 4 and 6). Rake 1 was mounted at ϕ = 33 deg, and rake 2 was mounted at ϕ = 213 deg. Before the flutter phase, rake 2 was moved to the position shown in Fig. 4 at ϕ = 147 deg. Rake 1 was adjustable in height, whereas rake 2 was fixed. Both rakes 1 and 2 were mounted such that measurements were made at a longitudinal position 0.5 in. forward of the aft edge of the shell.

Rake 3 was designed to investigate the boundary-layer growth from the blowing slot to the aft portion of the test shell by traversing the distance in finite steps. The rake was mounted at the free end of a circular support rod (Fig. 7). The support rod was cantilevered from a circular housing which allowed motion in the longitudinal direction. It was necessary to begin the test with the rake in the forward position, from which a spring system mounted in the tunnel plenum exerted a constant drag on the rake and support rod. A remotely controlled high-pressure air cylinder controlled the motion of the support rod by moving a stop bar to strike or free a protrusion from the support rod. Photographs of the rake in the extreme positions are shown in Fig. 8. Because of the flexibility of the long cantilever section, some damage to the rake pressure probes nearest the body was incurred during tunnel flow start.

The test shell itself was a right-circular cylinder 16 in. in diameter and 16 in. long and began 96 in. aft of the model nose and 48 in. aft of the beginning of the cylindrical portion of the model. For the pressure phase,

24 static pressure orifices were drilled into a 0.020-in. shell. The flutter investigation used shell thicknesses of 0.0020, 0.0028, 0.0033, and 0.0039 in. The pressure differential across the shell was controlled by varying the internal pressure through remotely controlled solenoid valves. High-pressure, rubber bladders were used to seal the internal cavity and prevent pressure loss. A quick-acting valve made it possible to vent the cavity region to free-stream static, thus giving a zero pressure differential across the shell. Axial loading could be applied to the shell by inflating bladders which acted on the end rings of the shell (Fig. 5).

2.3 INSTRUMENTATION

Weight flow of nitrogen injected into the boundary layer was computed in two ways. Two dynamic transducers mounted on either side of a sharp-edged orifice plate were used to measure the weight flow to the model immediately after the gas left the heaters. A pressure transducer in the manifold in the model was used to compute the flow into the free stream, assuming that the exit slot was choked. In general, the measurements made by the two methods differed by less than 0.02 lb/sec.

2.3.1 Pressure Phase

Pressure lines from the model orifices and boundary-layer rakes were routed to pressure transducers in the test section plenum chamber, the signals of which were digitized and reduced to pressure coefficient or boundary-layer parameters by a digital computer. Four static orifices near the nose of the model and four at the rear edge of the boundary-layer control section were located at 0-, 90-, 180-, and 270-deg roll positions and were used to orient the model at zero angle of attack. Twenty-four static orifices were installed in the test shell at the 0-, 90-, 180-, and 270-deg positions with six orifices in each meridian (Fig. 5).

Twenty-nine total pressures were measured from the three boundary-layer rakes (Fig. 6). Rakes 1 and 3 had static probes on the rakes, but rake 2 used a static reference pressure measured on the model surface.

Pressures inside the sealing (radial) bladders and the loading (axial) bladders were recorded, as were pressures within the boundary-layer system. Pressure measurements within the model cavity region were obtained on a dynamic transducer and by the tunnel pressure equipment. A dynamic pressure transducer was mounted in the boundary-layer control

section to measure the unsteady pressure on the model surface immediately forward of the test shell. Tabulated values for all of the measurements described were printed on-line, and selected pressures were recorded on magnetic tape. The position of the radially moveable rake was obtained from the output of a potentiometer.

2.3.2 Flutter Phase

For the flutter phase the pressure shell was replaced with thinner shells. With the exception of the 24 static orifices in the pressure shell, the instrumentation as described in Section 2.3.1 for the pressure phase was retained for the flutter phase. In addition, three mutual inductance proximity sensors were utilized to monitor the movement of the shell. The sensors measured both static and dynamic displacement of the shells. One sensor was fixed and served as a reference. Of the remaining two, one could move longitudinally only, and the other moved longitudinally and circumferentially. Longitudinal movement was 12 in., and circumferential movement was approximately 315 deg. The sensor positions were indicated by two potentiometers.

The sensors operated without contacting the shell surface with maximum output of approximately 4 v occurring when the shell (or calibration) surface was far away. The output decreased as the metal neared the sensor head. The signals from these sensors were recorded on magnetic tape, and root-mean-square and static displacements were tabulated for each test point.

SECTION III
TEST PROCEDURE

3.1 PRESSURE PHASE

The purpose of the pressure phase was to determine the effects of varying model parameters on the flow characteristics in the vicinity of the test shell. Changes in the static pressure distribution and boundary-layer profiles, caused by variation in the boundary-layer blowing, shell cavity pressure, tunnel Mach number, and total pressure, were investigated.

As flow was established and test conditions achieved, static pressure data and boundary-layer velocity profiles were obtained for zero boundary-layer blowing and nominal shell differential pressure, Δp_c, of 1 psi. Next, boundary-layer control (BLC) was added and data again taken for several blowing rates. Changes in tunnel total pressure were then made for the

same Mach number, and the process was repeated. At selected points while all other parameters were constant, the shell differential pressure was varied and data obtained to measure this effect on the external flow characteristics.

The traversing rake (rake 3) was operated for each Mach number. The most expedient method for using the traversing rake was to begin with the rake in the forward position and vary the tunnel total pressure, holding Mach number constant. The air-valve was actuated, releasing the yoke, and the spring force on the support rod caused the rake to slide back to the next position where a mechanical stop contacted the opposite arm of the yoke (Fig. 7). Again tunnel total pressure was varied. This process was repeated until all 12 positions of the rake had been covered. Other data were taken during the operation of the traversing rake to determine the effect of the rake and support rod on these measurements.

3.2 FLUTTER PHASE

Test conditions were achieved with the tunnel at a low total pressure and specified Mach number with Δp_c approximately 2.5 psi. Monitoring of the sensor outputs on an oscilloscope showed points at which the shell motion appeared to increase as the total pressure was increased. At these points, shell cavity pressure was adjusted to change the differential shell pressure within a range from 0 to 3.5 psi in an attempt to induce shell flutter. If no flutter occurred, compressive longitudinal loading up to 200 lb was applied to the shell by the axial bladders, and the differential shell pressure was again varied. During these investigations the moveable sensors were spanned several times to check the deformation of the shell.

3.3 PRECISION OF MEASUREMENTS

The uncertainties in setting and maintaining tunnel conditions are as follow:

Mach number	±0.005
Total pressure	±5 psf
Total temperature	±5°F
Angle of attack	±0.1 deg

The longitudinal variation of Mach number along the tunnel centerline has a maximum value of ±0.02.

The uncertainties associated with the tunnel pressure measuring system yield uncertainties in the pressure-coefficient data as follow:

M_∞	Re/ft x 10^{-6}	ΔC_p
2.20	0.564	0.0094
↓	1.546	0.0032
3.00	0.560	0.0102
↓	1.289	0.0044

SECTION IV
RESULTS

4.1 PRESSURE PHASE

The pressure coefficients shown in Fig. 9 were computed from measurements at the static orifices in the test shell for Mach numbers 2.20 and 3.00, respectively. The large pressure increase near the aft end of the shell in the 270-deg meridian is attributable to the traversing rake interference. The dotted line represents a characteristics solution for inviscid fluid and no mass addition. The zero-blowing results for both Mach numbers agree well with the characteristics solutions. Although this characteristics solution is good for zero blowing only, it has been added to all plots as a basis for comparison. Addition of mass flow to the boundary layer by blowing had little effect on the pressure coefficients, although the tendency was to decrease the pressures slightly. The variation in pressure along the shell may be caused by small buckles in the shell or local flow disturbances.

The boundary-layer profiles in Fig. 10 for Mach numbers 2.20 and 3.00 show the effect of blowing for different Reynolds numbers. The profiles with blowing show large distortions, either as straight or reverse curvature sections of the profiles. An examination of the profiles indicates that some leakage into the boundary layer was present for some of the zero-blowing cases. Data indicate leakage rates to 0.04 lb/sec could have been possible for some zero-blowing cases. While this small amount of blowing affected the pressure data somewhat, the main effect was felt in the dynamic aspects, as will be mentioned later.

The boundary-layer thicknesses were computed from the profiles in Fig. 10 and are shown in Fig. 11. For the case of nominal zero blowing, the boundary-layer thickness increases with rising Reynolds number and then approaches constant values of 0.8 and 1.4 in. for Mach numbers 2.20 and 3.00, respectively. These tendencies are contrary to turbulent

theory, which predicts an inverse relation between thickness and Reynolds number; however, no explanation for the disparity other than the possibility of BLC leakage is available. Blowing increased the boundary-layer thickness significantly, and for low Reynolds numbers, the thicknesses exceeded the boundary-layer rake height, as denoted by the undefined regions. As Reynolds number increases, the thicknesses become smaller.

The displacement thicknesses presented in Fig. 12 are based on measurements from the traversing rake as the rake was moved from the blowing slot (x = -25.13 in.) to the aft edge of the shell. Some trouble was experienced with this rake, including probe damage as the rake beat against the model before achievement of supersonic flow. Nevertheless, the general nature of the boundary-layer growth along the model may be ascertained. The data of Fig. 12c show much variation, which can be attributed in part to the movement of and damage to the traversing rake.

4.2 FLUTTER PHASE

Test conditions and ranges of variations for the control conditions are shown in Table I. Four shells of thicknesses 0.0020, 0.0028, 0.0033, and 0.0039 in. were tested. The 0.0033- and 0.0039-in. shells did not exhibit flutter tendencies during testing. The 0.0033-in. shell was loaded in compression to approximately 200 lb, at which point the shell buckled, causing a loss of pressurization in the cavity. When the shell was then vented to static pressure, it reinflated itself and remained intact until tunnel flow breakdown destroyed the shell at the end of the test period.

TABLE I

SUMMARY OF TEST CONDITIONS

M_∞	p_{t_∞}, psf	q_∞, psf	$Re_{/ft} \times 10^{-6}$	$\bar{F}$	h, in.	Δp_c, psi	FLUTTER	LOAD, lb
2.20	1400	443	1.710	15.4	0.0039	2.03 to 2.11	NONE	NONE
3.00	549 to 1650	100 to 282	0.456 to 1.250	8.4 to 11.7	0.0033	0.01 to 2.84	NONE	NONE
2.60	753 to 1303	186 to 309	0.752 to 1.252	10.9 to 12.8	0.0033	-0.45 to 0.75	NONE	0 to 196
2.20	800 to 1501	253 to 476	1.004 to 1.880	12.8 to 15.8	0.0028	-0.97 to 0.53	DESTRUCTIVE	NONE
2.20	199 to 1566	64 to 501	0.252 to 1.920	13.0 to 25.9	0.0020	-0.75 to 3.60	LIMIT CYCLE	NONE

Oscillatory motions which may be described as destructive and nondestructive were encountered on the 0.0028- and 0.0020-in. shells, respectively. The 0.0028-in. shell failed during high amplitude oscillations lasting a few milliseconds at a tunnel total pressure of 1500 psf. The

differential pressure was approximately zero, and no compressive loading was applied at the time of the failure.

Testing of the 0.0020-in. shell resulted in a long period of limit cycle oscillations at a frequency near 1400 cps. The shell differential pressure was varied from 2.5 to 3.5 psi, and the limit cycle persisted for tunnel total pressures from 320 to 510 psf. Longitudinal and traverse sensor surveys along the interior of the model shell revealed that the motion was of an axisymmetric standing wave pattern with two nodes observed on the longitudinal scan. The motion of the shell was damped completely by the addition of boundary-layer blowing at a rate of 0.08 lb/sec. Blowing was initiated for a tunnel total pressure of 322 psf and was maintained at the same rates for total pressure increasing to approximately 1560 psf in an attempt to induce flutter with blowing. Although the random motion of the shell did increase in amplitude, no other flutter was encountered.

Because of the stabilizing effect of a very small amount of boundary-layer blowing on the 0.0020-in. shell, the possibility of stabilizing effects on previous shells caused by leakage of air into the boundary layer appears likely. The 0.0020-in. shell fluttered readily for zero-blowing cases but could not be made to flutter with blowing, even for total pressures to 1565 psf (Table II). Therefore, it is possible that previous shells, which did experience random motion but no flutter, could have been under the influence of a slight blowing rate, which critically affected the dynamic characteristics.

TABLE II

FLUTTER CONDITIONS

M_∞	p_{t_∞}, psf	q_∞, psf	$Re/ft \times 10^{-6}$	$\bar{F}$	h, in	Δp_c, psi
2.20	1500	476	1.842	13.5	0.0028	0.01
2.20	510	161	0.771	17.7	0.0020	1.84
2.20	504	160	0.758	17.6	0.0020	1.93
2.20	503	159	0.740	17.6	0.0020	2.15
2.20	498	158	0.722	17.5	0.0020	2.51
2.20	379	120	0.539	16.0	0.0020	2.67
2.20	379	120	0.528	16.0	0.0020	3.44
2.20	379	120	0.526	16.0	0.0020	3.58
2.20	373	118	0.515	15.9	0.0020	3 38
2.20	334	106	0.462	15.4	0.0020	3.09
2 20	323	102	0.444	15.2	0.0020	2.98
2.20	322	102	0.442	15.2	0.0020	2.88

SECTION V
CONCLUSIONS

The following conclusions are drawn from the results of this test:

1. The static pressure distribution appeared to change only slightly with boundary-layer blowing.
2. Blowing increased the displacement thickness significantly.
3. Divergent flutter oscillations were experienced on a 0.0028-in. shell at a differential pressure of approximately zero.
4. Limit cycle oscillations occurred on a 0.0020-in. shell. The addition of blowing eliminated this motion.

REFERENCES

1. Perkins, T. M. and Brice, T. R. "An Investigation of the Aeroelastic Stability of Thin Cylindrical Shells at Transonic Mach Numbers." AEDC-TR-66-93 (AD632829), May 1966.
2. Test Facilities Handbook (Sixth Edition). "Propulsion Wind Tunnel Facility, Vol. 5." Arnold Engineering Development Center, November 1966.
3. Nichols, J. H., Davis, M. W., and Garner, C. L., Jr. "Initial Aerodynamic Calibration Results for the AEDC-PWT 16-ft Supersonic Tunnel." AEDC-TDR-62-55 (AD273527), March 1962.
4. Nichols, J. H. "Supplemental Aerodynamic Calibration Results for the AEDC-PWT 16-ft Supersonic Tunnel." AEDC-TDR-64-76 (AD435732), April 1964.

APPENDIX
ILLUSTRATIONS

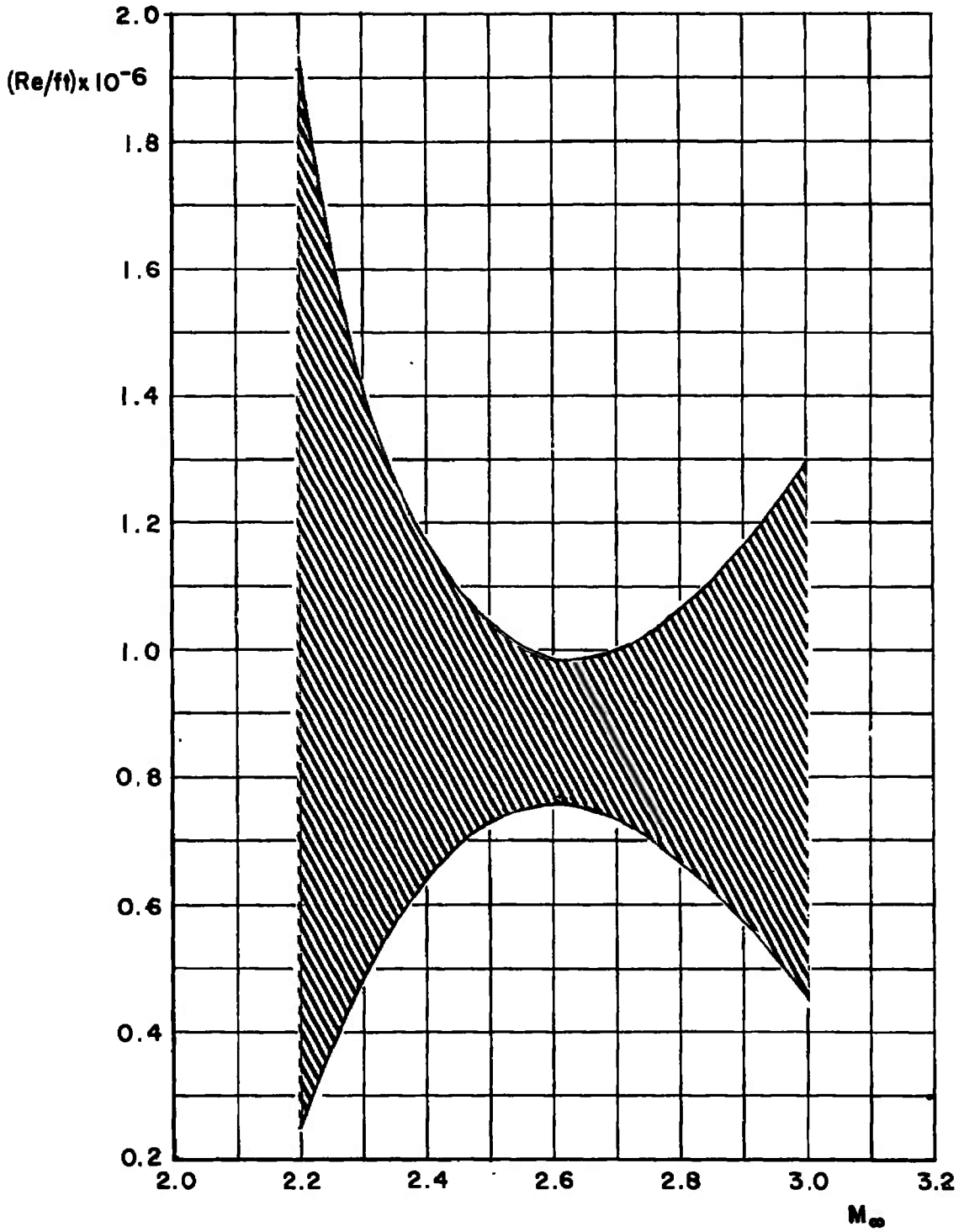

Fig. 1 Variations of Tunnel Reynolds Number with Mach Number

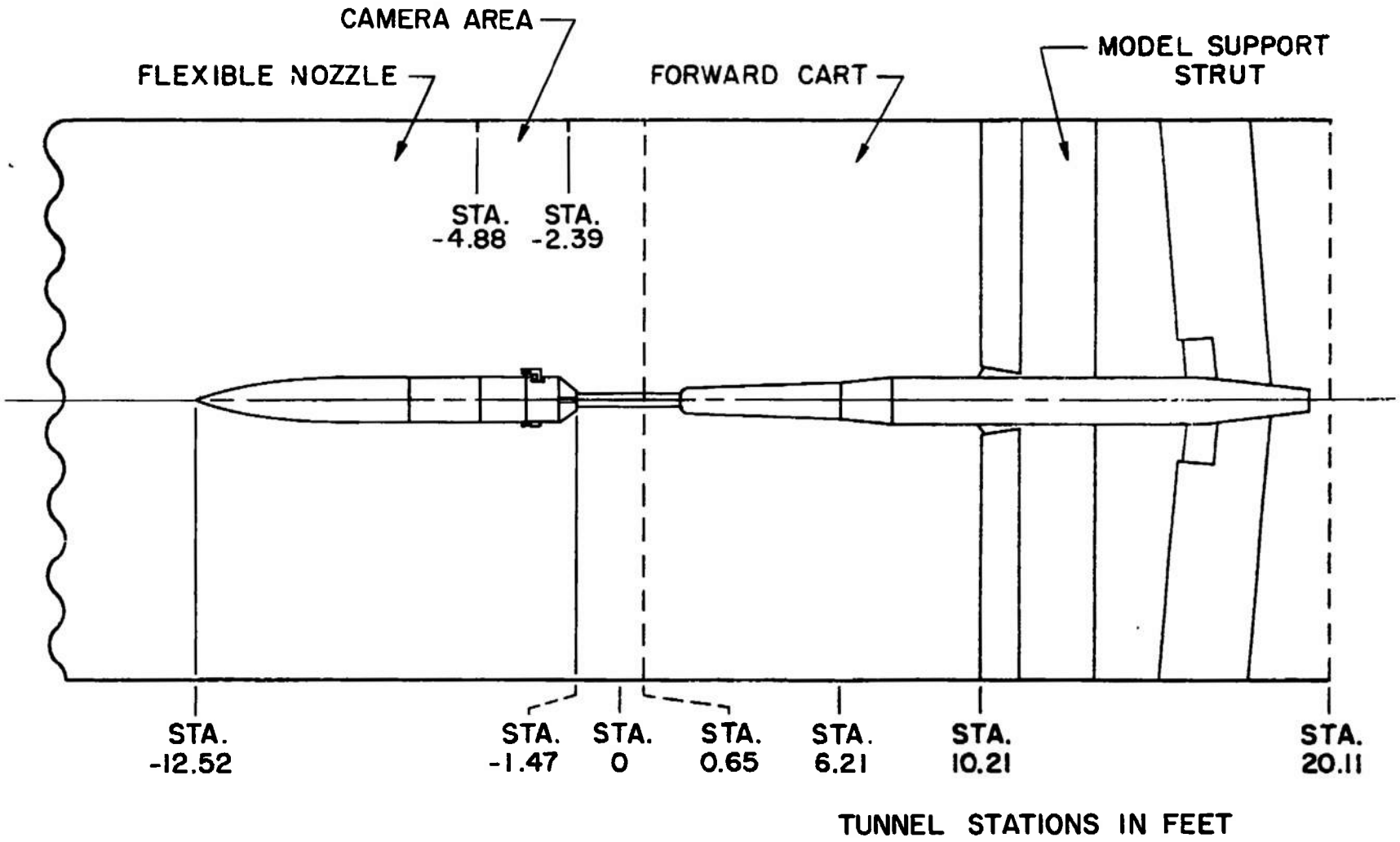

Fig. 2 Sketch of the Model in the Tunnel 16S Test Section

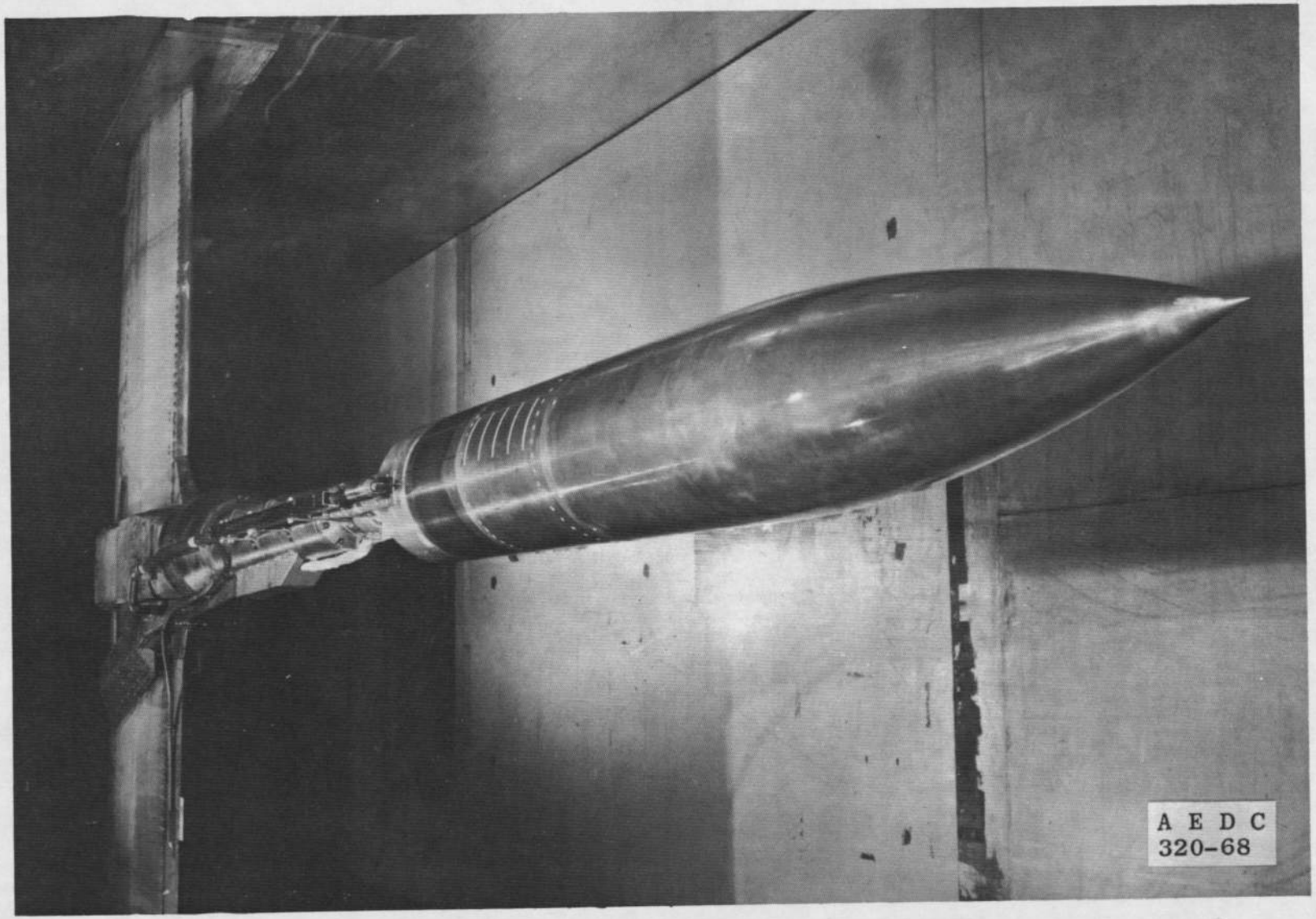

Fig. 3 Photograph of the Model Installed in the Tunnel 16S Test Section

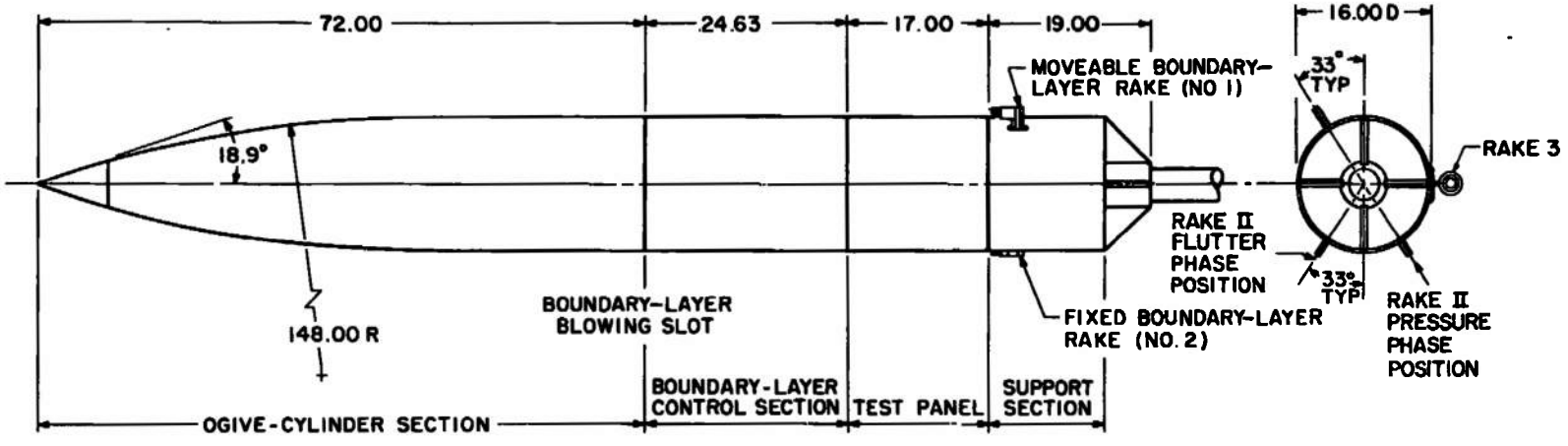

ALL DIMENSIONS IN INCHES

Fig. 4 Model Dimensions and Details

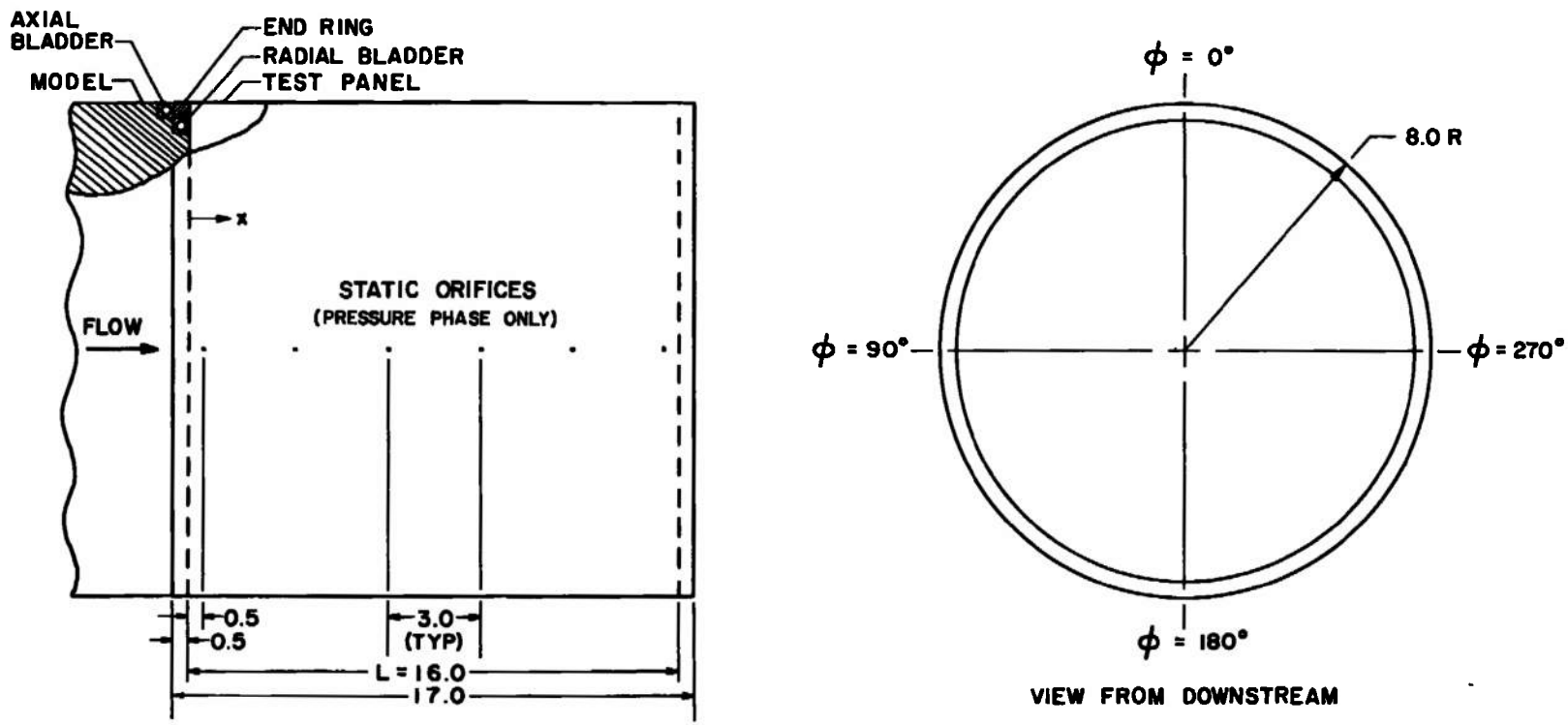

Fig. 5 Details of the Test Panel

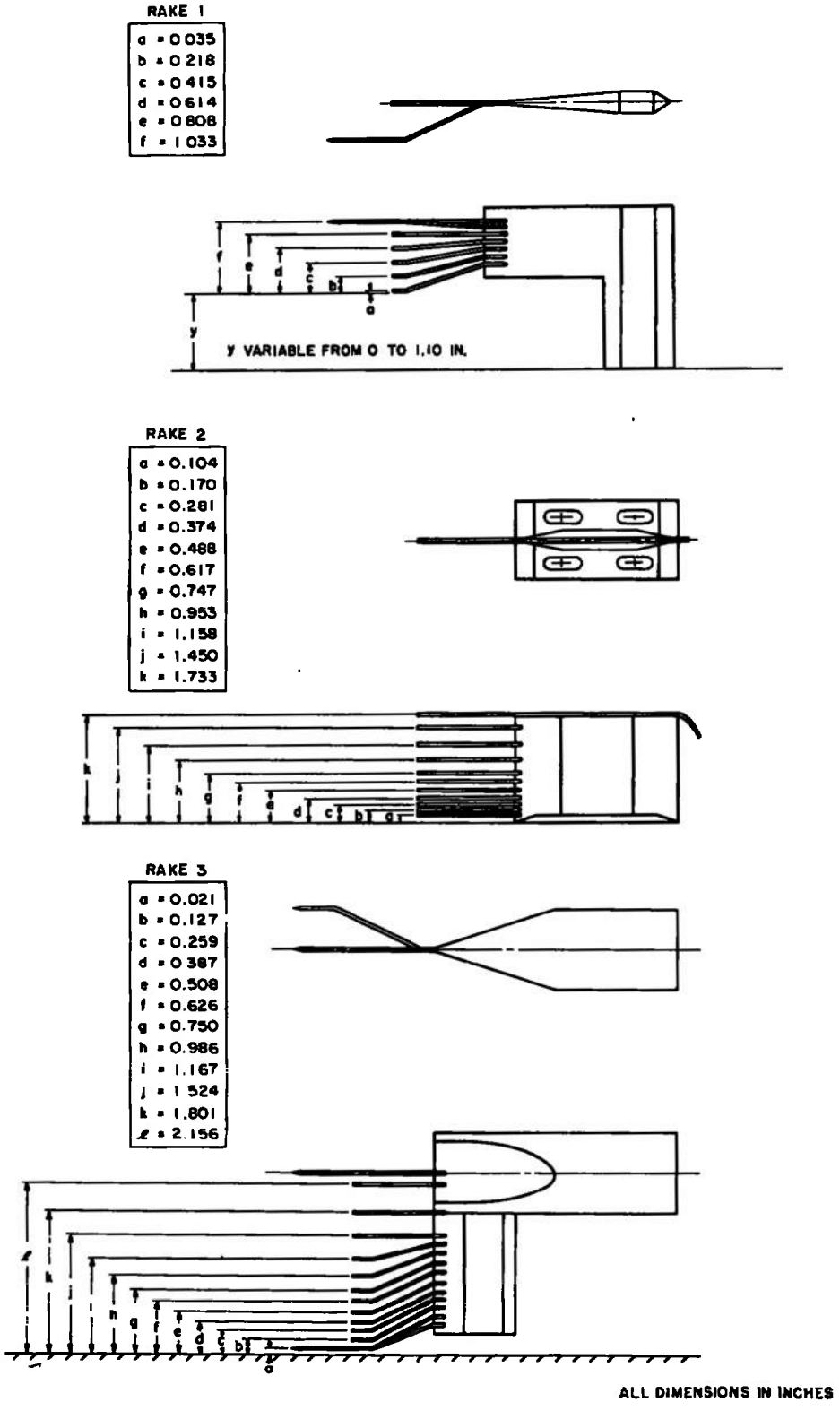

Fig. 6 Details of the Boundary-Layer Rakes

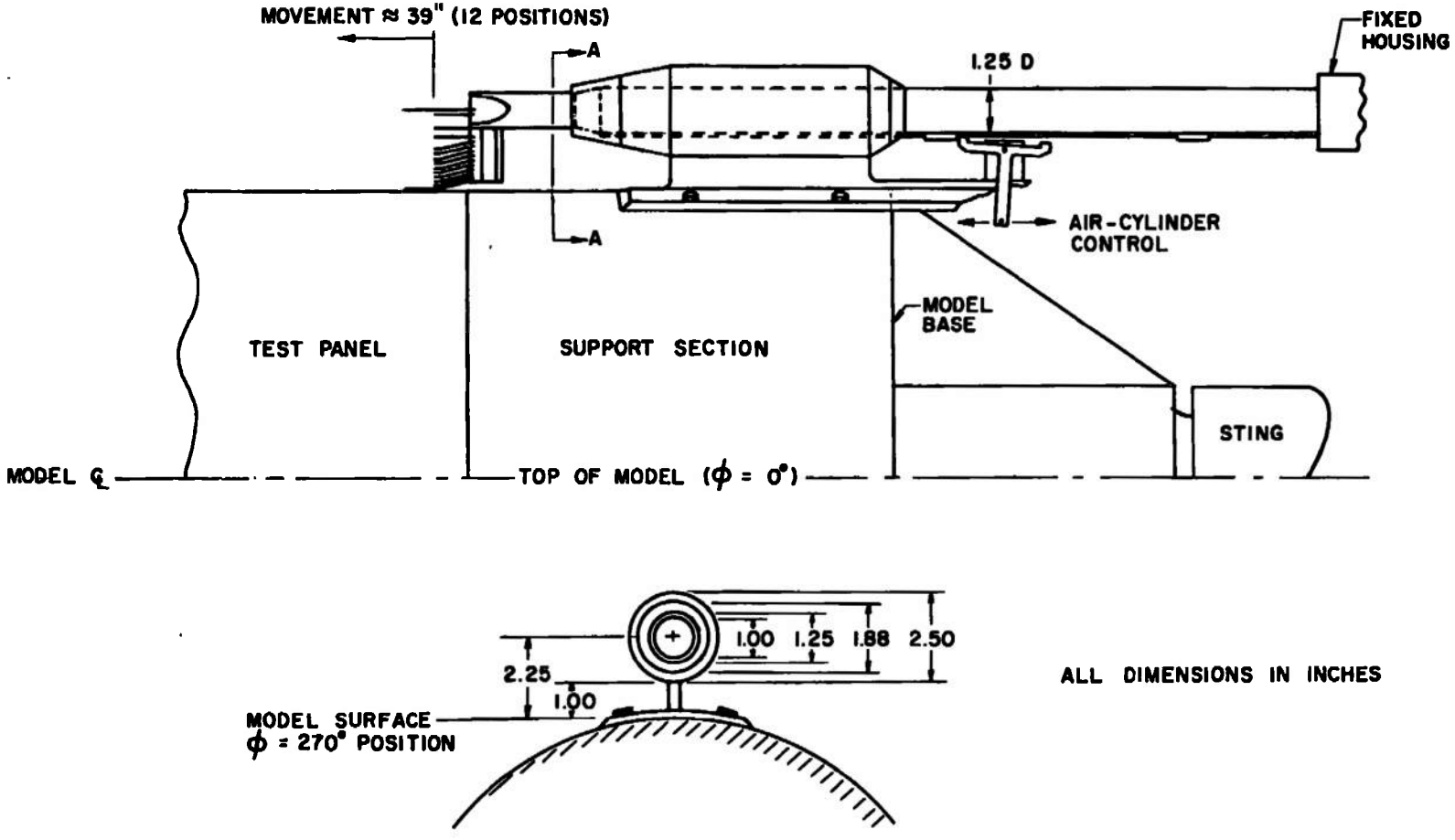

Fig. 7 Sketch of the Traversing Rake (Rake 3)

a. Forward Position

Fig. 8 Photographs of Rake 3

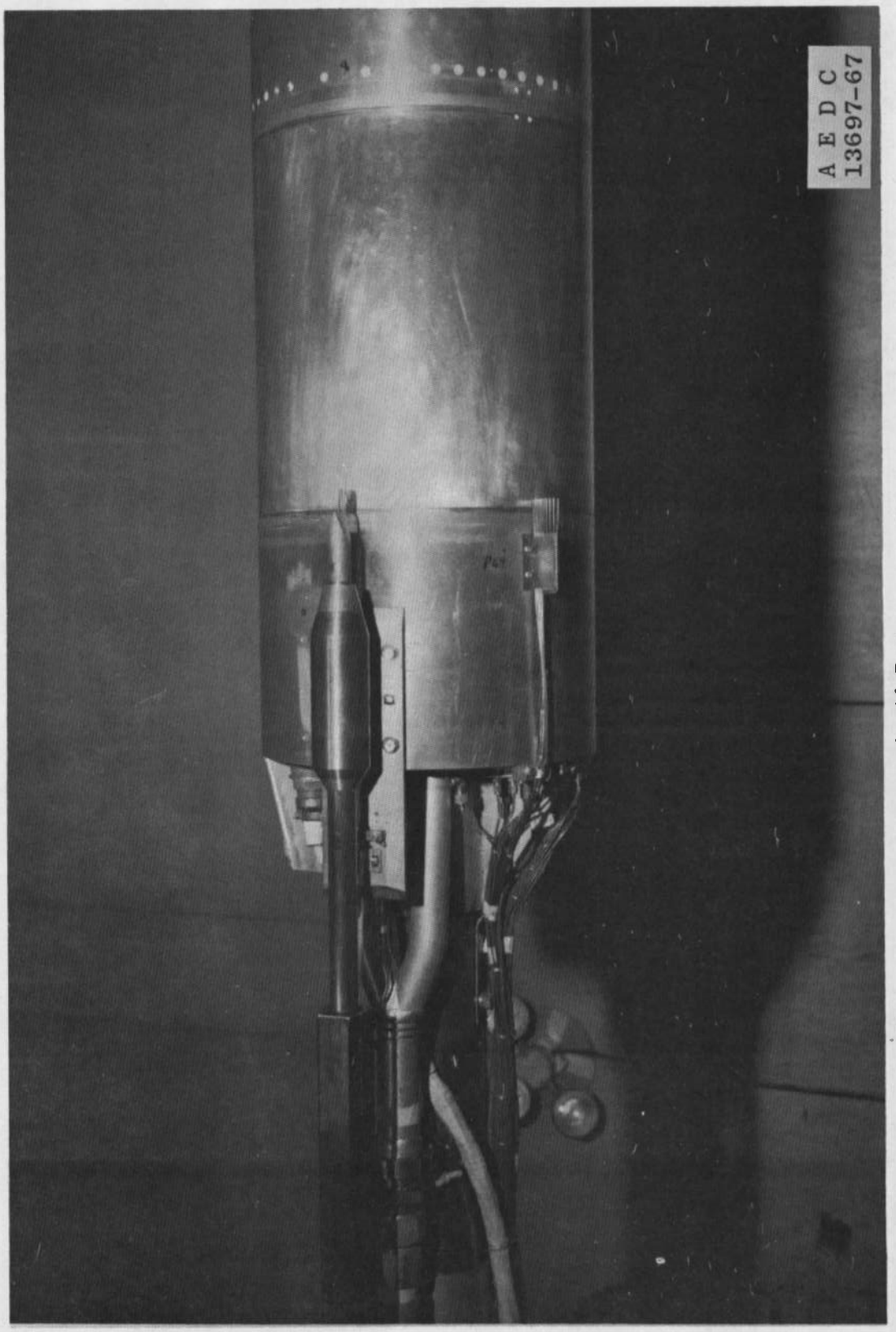

b. Aft Position
Fig. 8 Concluded

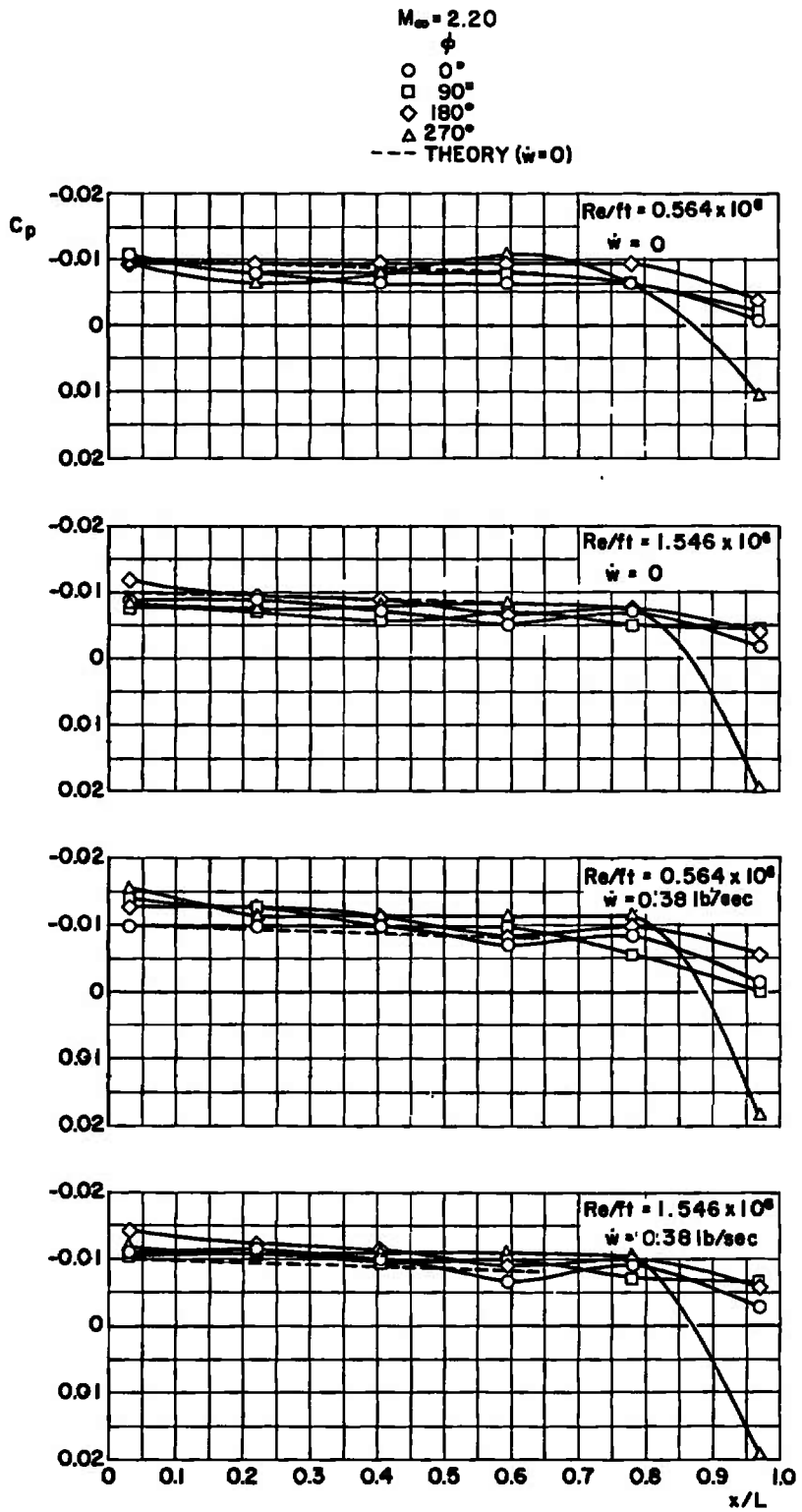

a. $M_{\infty} = 2.20$

Fig. 9 Variation of Pressure Coefficients on the Test Shell, with and without Boundary-Layer Blowing

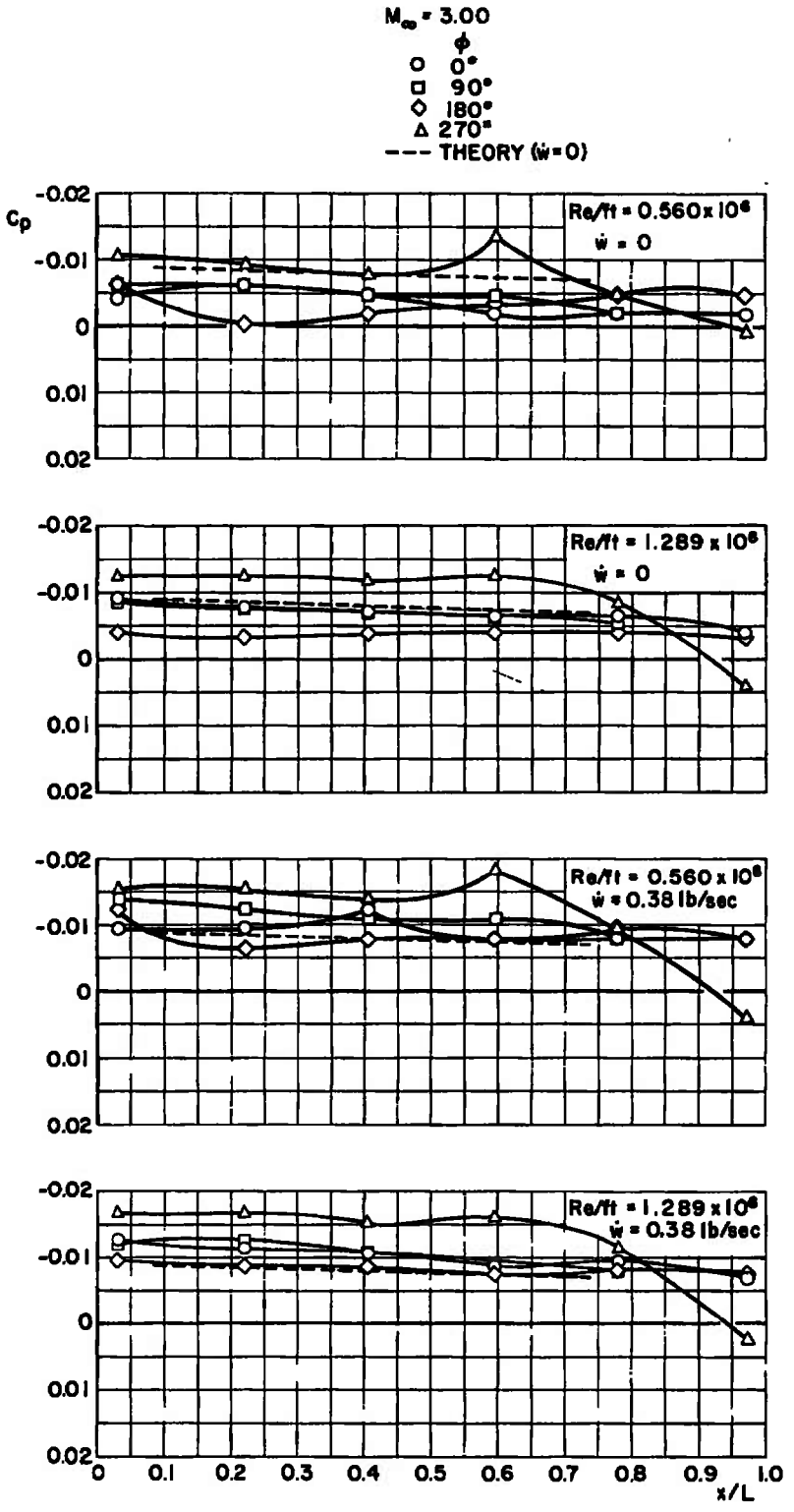

b. $M_\infty = 3.00$

Fig. 9 Concluded

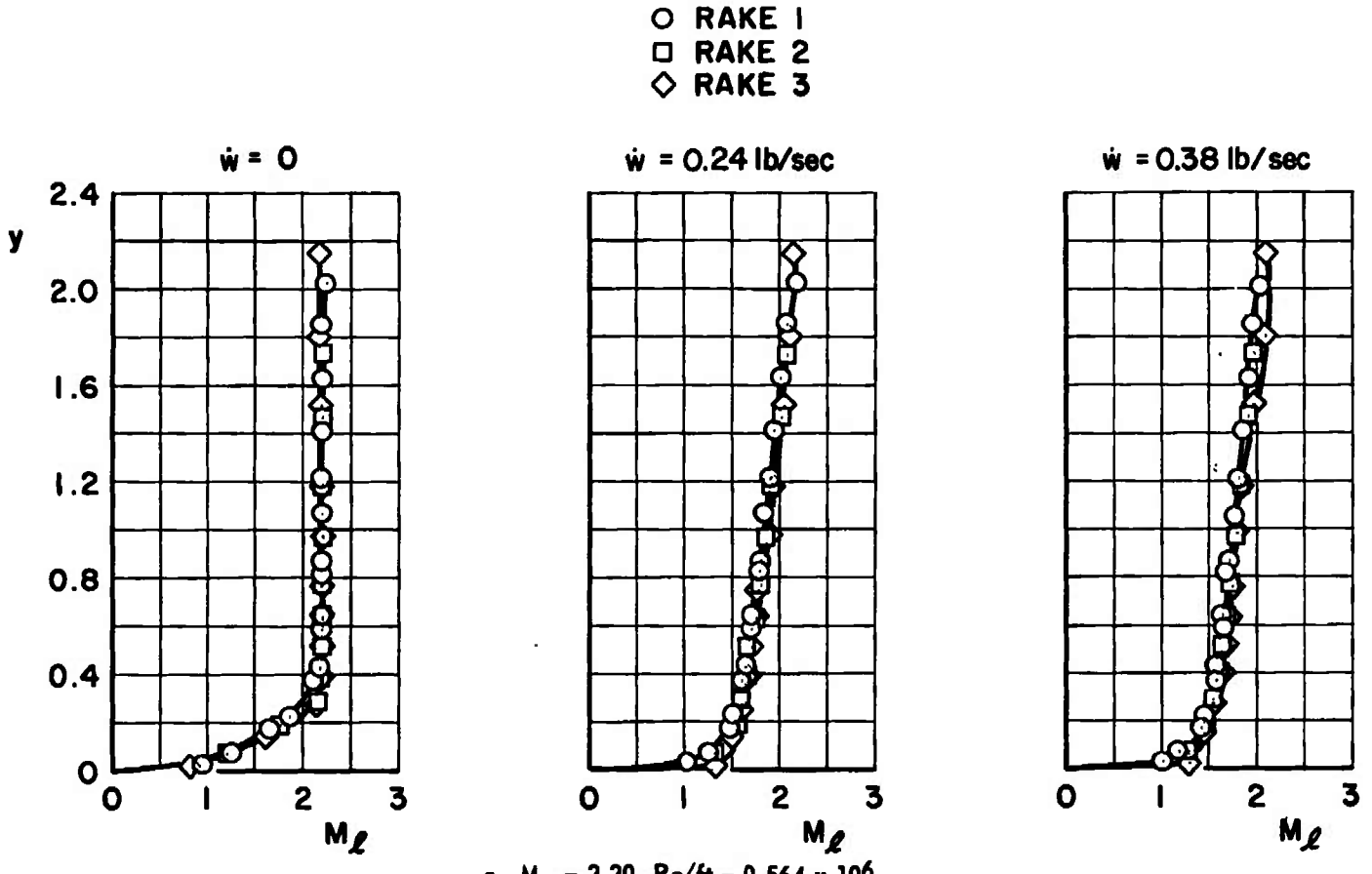

a. $M_\infty = 2.20$, Re/ft = 0.564×10^6

Fig. 10 Boundary-Layer Profiles at x/L = 1.00

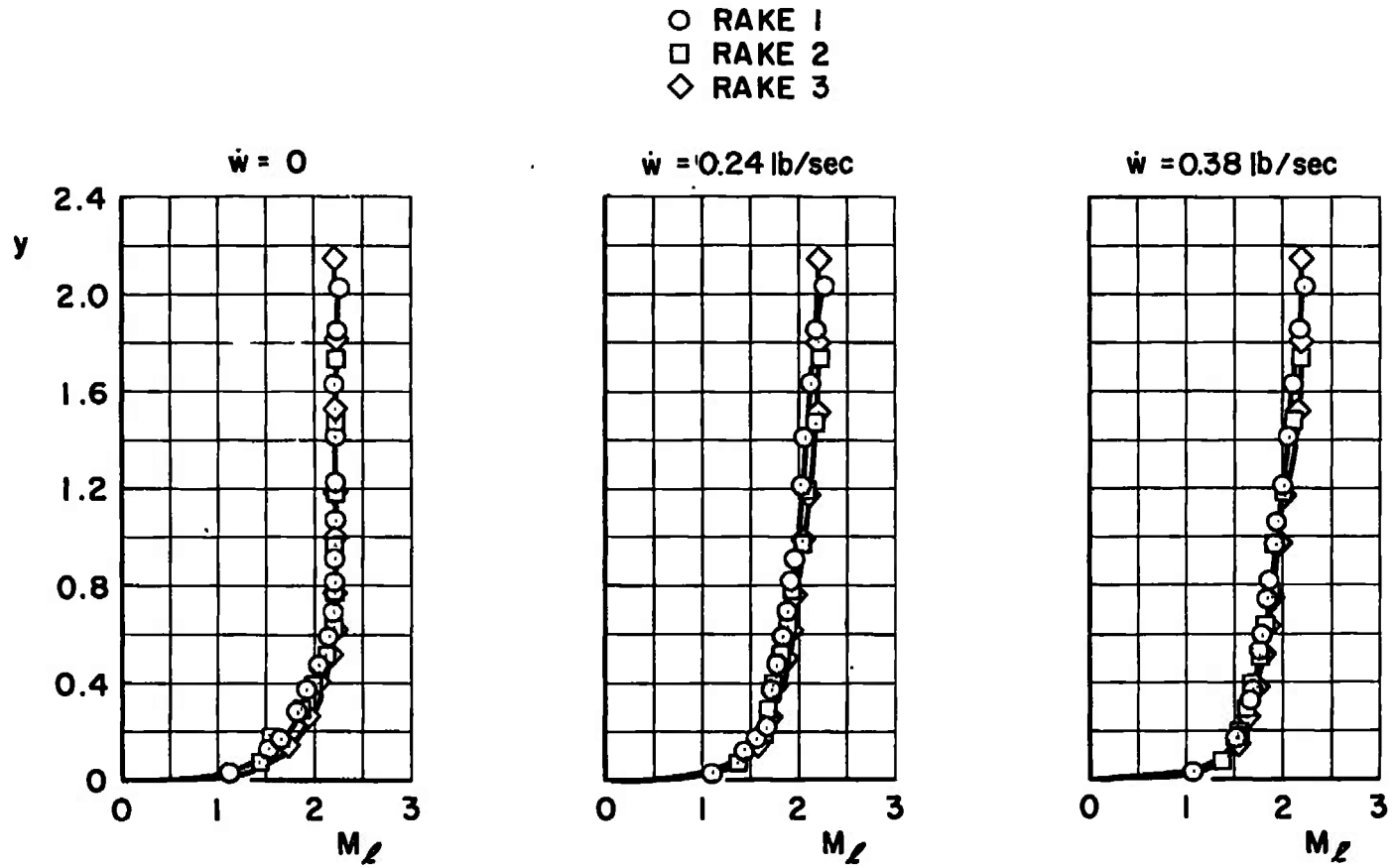

b. $M_\infty = 2.20$, Re/ft = 1.092×10^6

Fig. 10 Continued

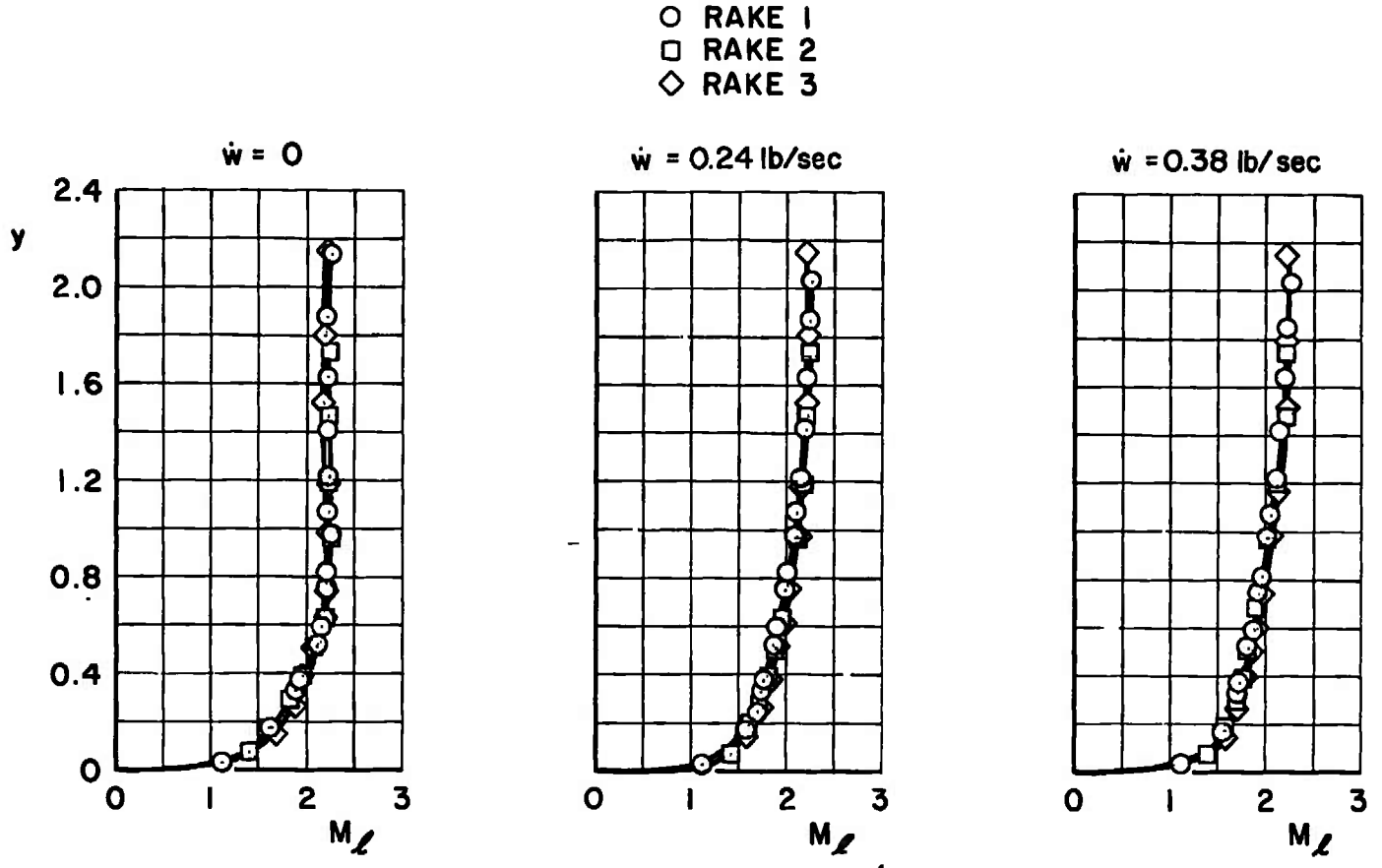

c. $M_\infty = 2.20$, Re/ft = 1.546×10^6

Fig. 10 Continued

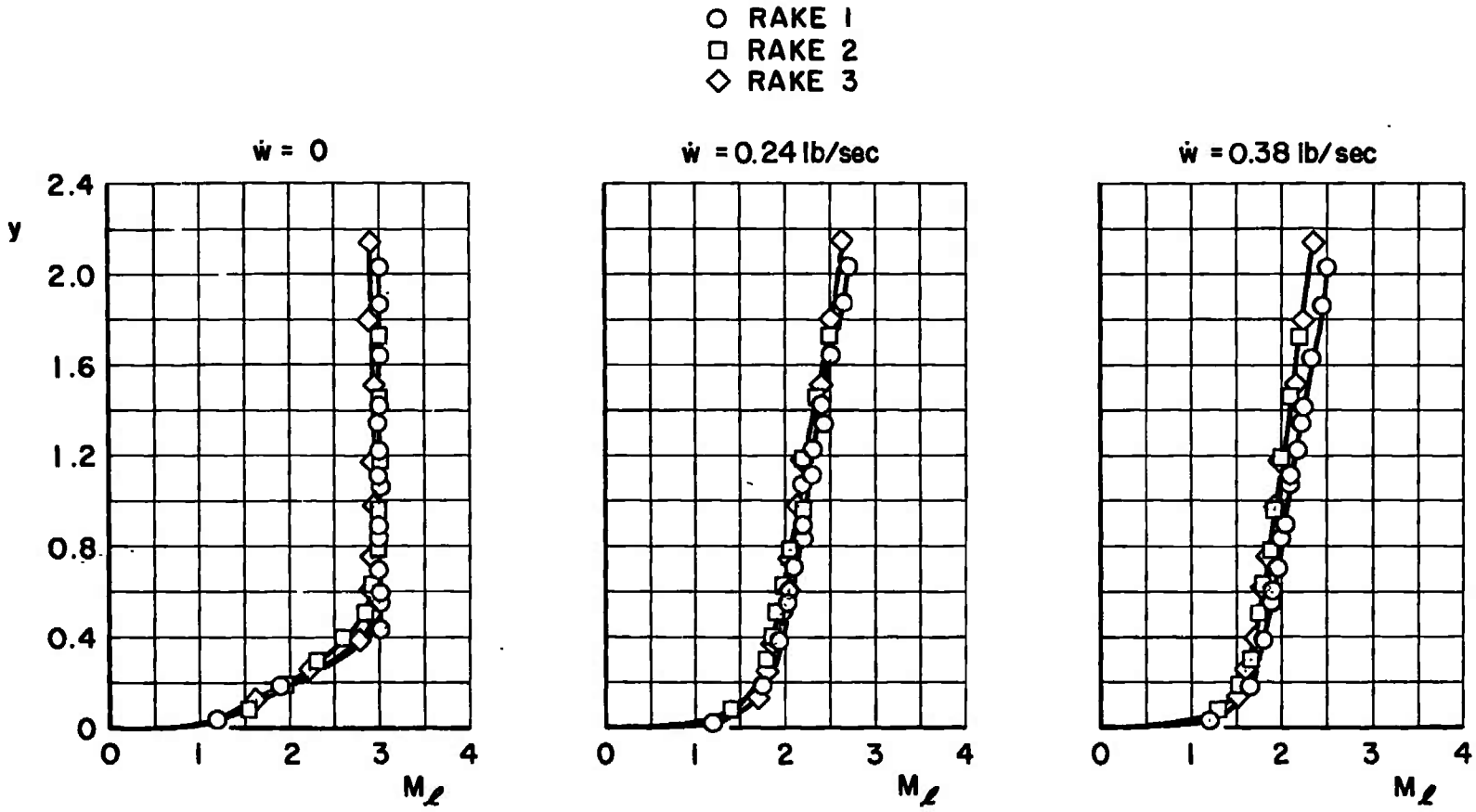

d. $M_\infty = 3.00$, $Re/ft = 0.560 \times 10^6$
Fig. 10 Continued

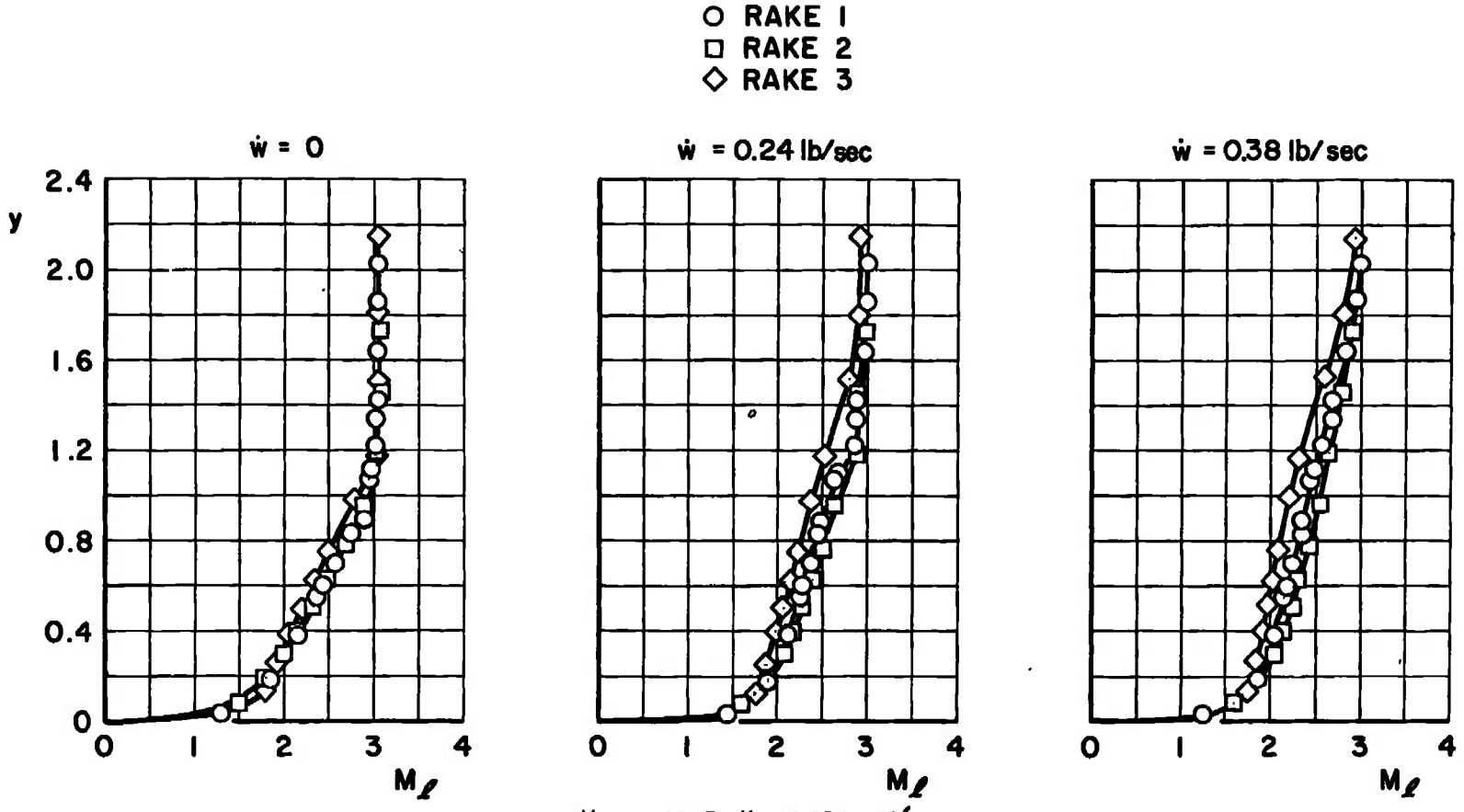

e. $M_\infty = 3.00$, $Re/ft = 0.994 \times 10^6$

Fig. 10 Continued

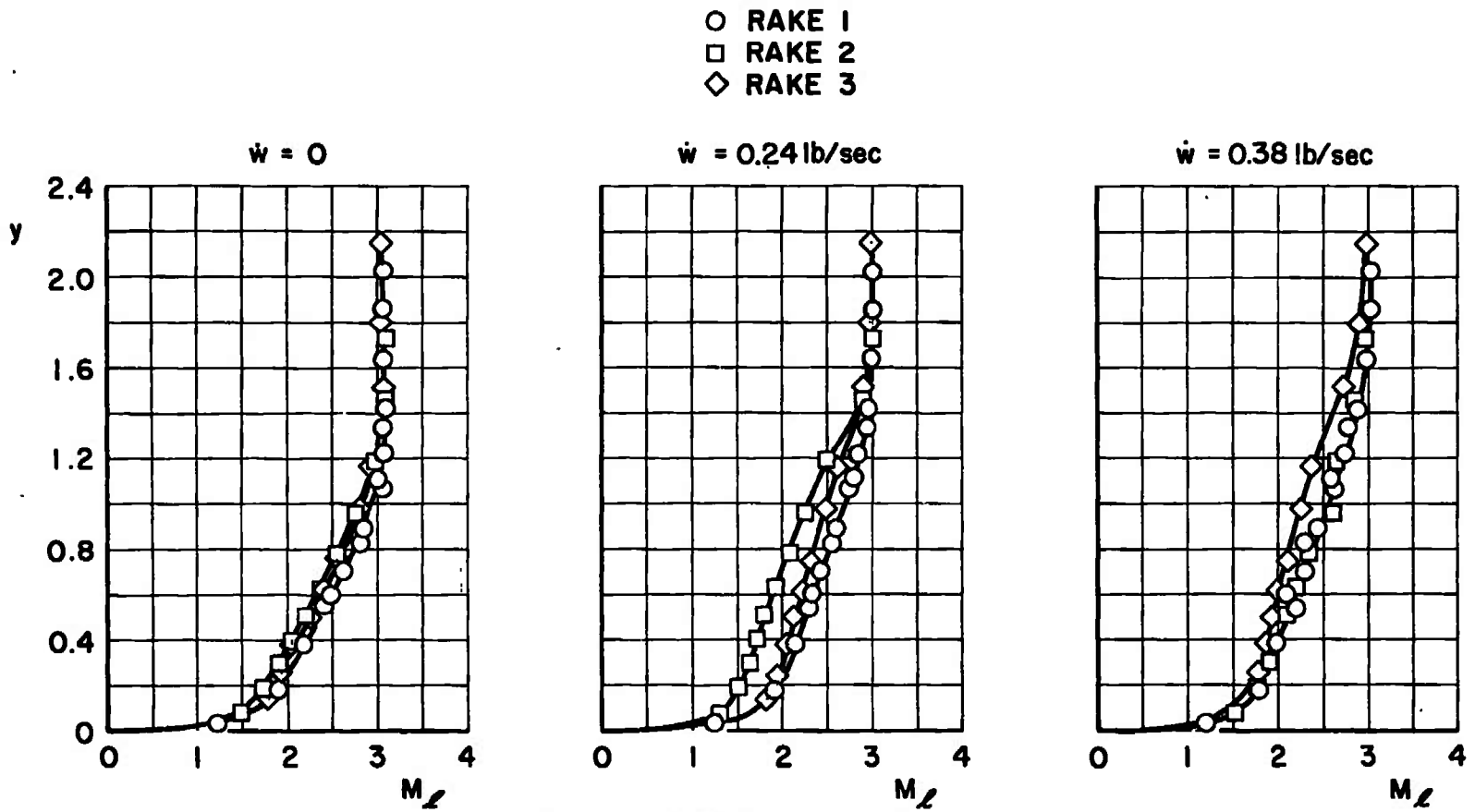

f. $M_\infty = 3.00$, $Re/ft = 1.289 \times 10^6$

Fig. 10 Concluded

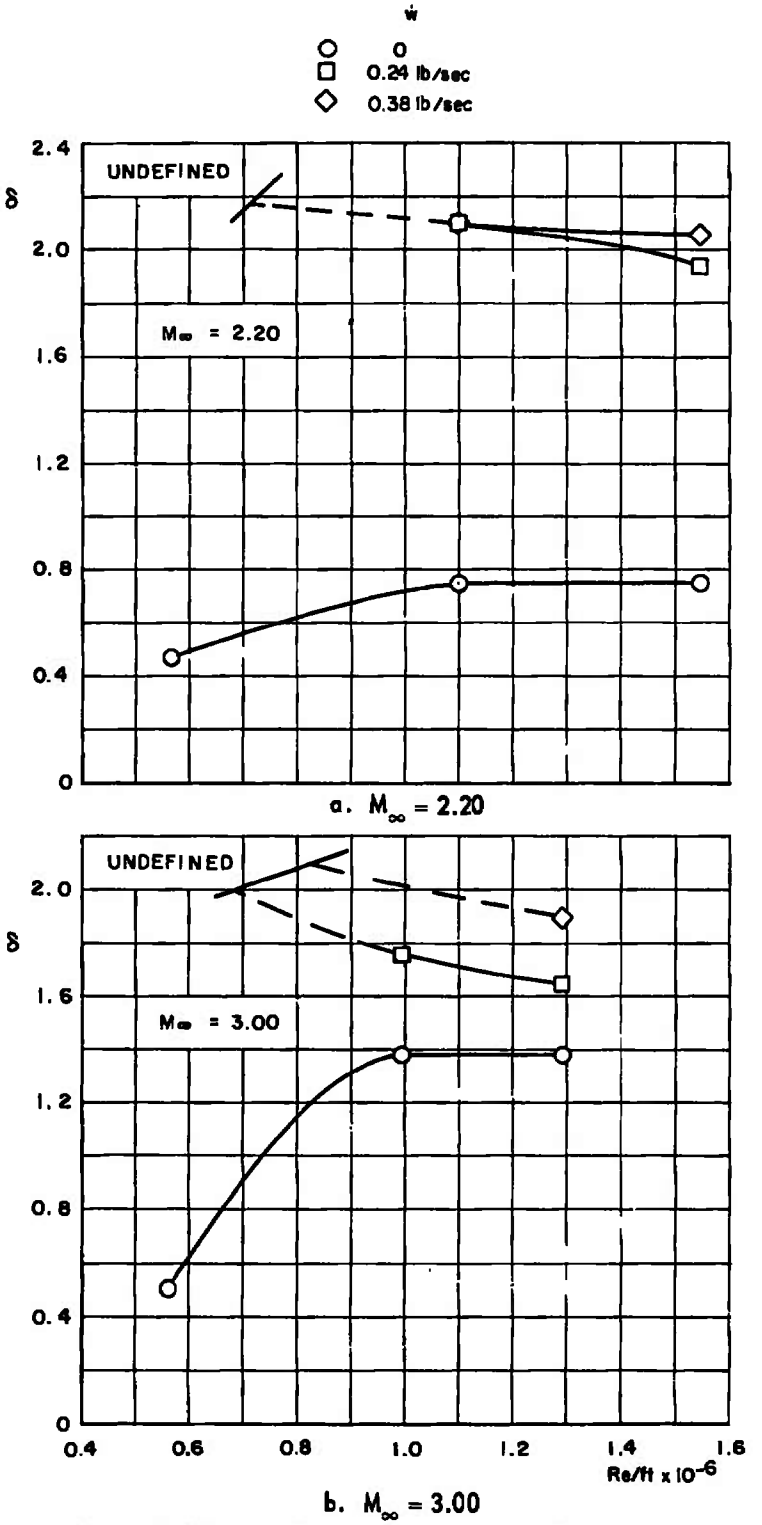

Fig. 11 Effect of Reynolds Number and Blowing on the Boundary-Layer Thickness at x/L = 1.00

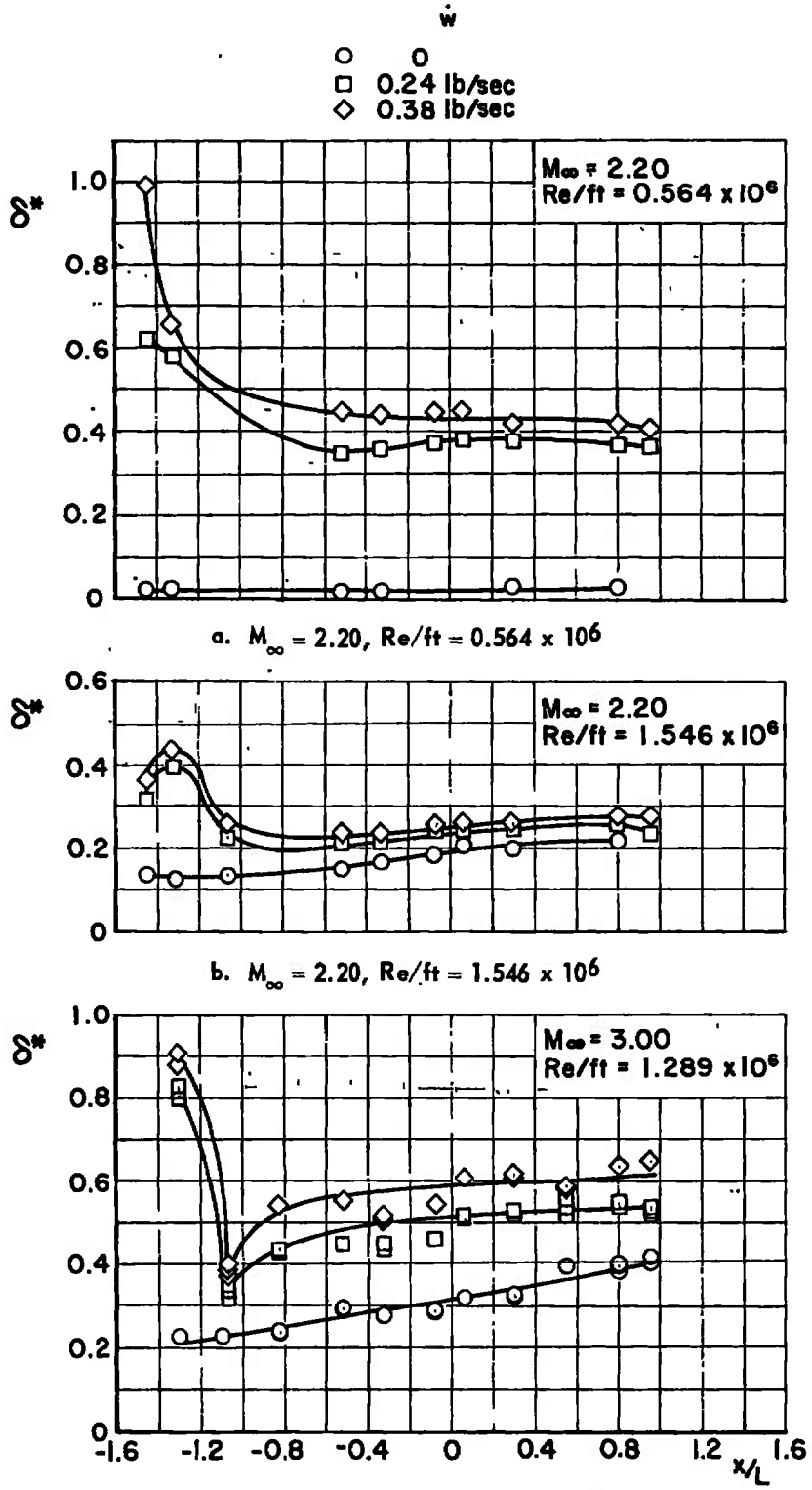

a. $M_\infty = 2.20$, $Re/ft = 0.564 \times 10^6$

b. $M_\infty = 2.20$, $Re/ft = 1.546 \times 10^6$

c. $M_\infty = 3.00$, $Re/ft = 1.289 \times 10^6$

Fig. 12 Variation of the Displacement Thickness along the Model Surface, with and without Boundary-Layer Blowing

UNCLASSIFIED
Security Classification

DOCUMENT CONTROL DATA - R & D

(Security classification of title, body of abstract and indexing annotation must be entered when the overall report is classified)

1. ORIGINATING ACTIVITY (Corporate author) Arnold Engineering Development Center, ARO, Inc., Operating Contractor, Arnold AF Station, Tennessee	2a. REPORT SECURITY CLASSIFICATION UNCLASSIFIED 2b. GROUP N/A

3. REPORT TITLE

AEROELASTIC STABILITY TESTS OF THIN CYLINDRICAL SHELLS AT SUPERSONIC SPEEDS

4. DESCRIPTIVE NOTES (Type of report and inclusive dates)
Final Report - October 24 through November 2, 1967, and January 15 through 19, 1968

5. AUTHOR(S) (First name, middle initial, last name)

T. R. Brice, ARO, Inc.

6. REPORT DATE	7a. TOTAL NO. OF PAGES	7b. NO. OF REFS
April 1968	38	4

8a. CONTRACT OR GRANT NO.	9a. ORIGINATOR'S REPORT NUMBER(S)
AF40(600)-1200	AEDC-TR-68-79
b. PROJECT NO. 9782	
c. Program Element 6144501F	9b. OTHER REPORT NO(S) (Any other numbers that may be assigned this report) N/A
d.	

10. DISTRIBUTION STATEMENT
This document is subject to special export controls and each transmittal to foreign governments or foreign nationals may be made only with prior approval of Air Force Office of Scientific Research (SREM), Arlington, Virginia 22209.

11. SUPPLEMENTARY NOTES	12. SPONSORING MILITARY ACTIVITY
Available in DDC.	Air Force Office of Scientific Research (SREM), Arlington, Virginia 22209

13. ABSTRACT

Dynamic characteristics of thin cylindrical shells were investigated for Mach numbers from 2.2 to 3.0. The Reynolds number based on the model diameter varied from 0.34 to 2.58 million. Limit cycle oscillations in a standing wave mode occurred on a 0.0020-in. shell at Mach number 2.2. The limit cycle motion was damped completely by blowing air into the boundary layer at a very low rate. A 0.0028-in. shell was destroyed during high amplitude oscillations at Mach number 2.2. Pressure distribution and boundary-layer measurements were also made.

This document is subject to special export controls and each transmittal to foreign governments or foreign nationals may be made only with prior approval of Air Force Office of Scientific Research (SREM), Arlington, Virginia 22209.

This document has been approved for public release and sale; its distribution is unlimited. PERTAB 72-19, Dtd 10Ct, 72.

DD FORM 1 NOV 65 1473

UNCLASSIFIED
Security Classification

14. KEY WORDS	LINK A ROLE	LINK A WT	LINK B ROLE	LINK B WT	LINK C ROLE	LINK C WT
cylindrical shells						
stability testing						
standing wave modes						
limit cycle oscillations						
supersonic flow						

2. Shells -- Stability

3 " -- --

4 " -- -- Supersonic flow

1 - 2